Monthly Notices
of the
ROYAL ASTRONOMICAL SOCIETY

MNRAS **490,** 4230–4236 (2019)
Advance Access publication 2019 September 19

doi:10.1093/mnras/stz2602

Transit timing variations in the WASP-4 planetary system

John Southworth,[1★] M. Dominik,[2] U. G. Jørgensen,[3] M. I. Andersen,[4] V. Bozza,[5,6] M. J. Burgdorf,[7] G. D'Ago,[8] S. Dib,[9,10] R. Figuera Jaimes,[11] Y. I. Fujii,[3,4,12] S. Gill,[1,13] L. K. Haikala,[14] T. C. Hinse,[15] M. Hundertmark,[10] E. Khalouei,[16] H. Korhonen,[17] P. Longa-Peña,[18] L. Mancini,[10,19,20,21] N. Peixinho,[22] M. Rabus,[23,24] S. Rahvar,[16] S. Sajadian,[25] J. Skottfelt,[26] C. Snodgrass,[27] P. Spyratos,[1] J. Tregloan-Reed,[18] E. Unda-Sanzana[18] and C. von Essen[28]

Affiliations are listed at the end of the paper

Accepted 2019 September 11. Received 2019 September 6; in original form 2019 July 19

ABSTRACT

Transits in the planetary system WASP-4 were recently found to occur 80 s earlier than expected in observations from the *TESS* satellite. We present 22 new times of mid-transit that confirm the existence of transit timing variations, and are well fitted by a quadratic ephemeris with period decay $\mathrm{d}P/\mathrm{d}t = -9.2 \pm 1.1$ ms yr^{-1}. We rule out instrumental issues, stellar activity, and the Applegate mechanism as possible causes. The light-time effect is also not favoured due to the non-detection of changes in the systemic velocity. Orbital decay and apsidal precession are plausible but unproven. WASP-4 b is only the third hot Jupiter known to show transit timing variations to high confidence. We discuss a variety of observations of this and other planetary systems that would be useful in improving our understanding of WASP-4 in particular and orbital decay in general.

Key words: stars: activity – stars: fundamental parameters – stars: individual: WASP-4.

1 INTRODUCTION

Thousands of transiting planets are currently known. Under the assumption of Keplerian motion, the transits are expected to recur with a strict periodicity. However, there is a range of phenomena that might change this behaviour, including stellar activity (Oshagh et al. 2013), gravitational interactions (Holman & Murray 2005), the light-time effect in multiple systems (Woltjer 1922), and orbital decay due to tides (Birkby et al. 2014). Because of this, extensive efforts have been devoted to the detection of transit timing variations (TTVs; e.g. Gibson et al. 2010; Harpsøe et al. 2013; Maciejewski et al. 2018b). Many examples have been found for small planets observed using the *Kepler* satellite (Mazeh et al. 2013) but only *two* detections have been made for a planet outside the *Kepler* field. Maciejewski et al. (2016) used transit timing measurements taken over 3.3 yr to find a quadratic term in the orbital ephemeris of WASP-12 to a significance of 5σ (see also Patra et al. 2017; Maciejewski et al. 2018b), and WASP-47 b shows sinusoidal TTVs due to the presence of two smaller short-period planets (Becker et al. 2015).

In this work we show that WASP-4 b (Wilson et al. 2008) is the third giant planet known to exhibit detectable TTVs, with a significance of 8.4σ. This confirms preliminary suggestions from Bouma et al. (2019, hereafter B19) based on data from the *TESS* satellite (Ricker et al. 2015). Baluev et al. (2015) have also claimed a tentative detection of TTVs in WASP-4, in the form of a sinusoidal variation with a period near 5 d; we do not confirm this detection. When needed, we will adopt the physical properties of the WASP-4 system given by Southworth (2012). In brief, the planet has mass 1.25 $\mathrm{M_{Jup}}$ and radius 1.36 $\mathrm{R_{Jup}}$, and is on a 1.338 d orbit around a star of mass 0.93 $\mathrm{M_{\odot}}$ and radius 0.91 $\mathrm{R_{\odot}}$. The star's effective temperature is 5500 K (Mortier et al. 2013) and it shows magnetic activity in the form of dark star-spots (Sanchis-Ojeda et al. 2011). No companion stars have been found in high-resolution imaging studies (Ngo et al. 2015; Evans et al. 2016) and no long-term trend in systemic velocity has been identified (Knutson et al. 2014).

2 OBSERVATIONS

We have been monitoring transits in the WASP-4 system for approximately a decade using the Danish 1.54 m telescope and DFOSC imager at ESO La Silla, as a side project of the MiNDSTEp Consortium (Dominik et al. 2010). Four transits observed in the 2008 season were presented in Southworth et al. (2009b), and we also observed one transit in 2009, two in 2011, three in 2015, three in 2016, two in 2017, and three in 2018. All observations were obtained through a Cousins *R* filter with the CCD unbinned and the telescope significantly defocused to enhance the photometric

★ E-mail: astro.js@keele.ac.uk

precision (Southworth et al. 2009a). The scatters of the data sets versus transit fits (see below) range from 0.54 to 1.03 mmag with cadences of typically 140 s.

We also observed one transit in the WASP-4 system using the NTT and EFOSC2 imager (Buzzoni et al. 1984) with an SDSS r filter (ESO filter #784) on the night of 2011 October 21. The telescope was defocused, the CCD was not binned, and only one comparison star was used due to the small field of view. The light curve is of very high quality (see Tregloan-Reed & Southworth 2013), with a scatter of 0.47 mmag.

Finally, we observed three transits using the SAAO 1.0 m telescope at Sutherland, South Africa: two in 2016 and one in 2019. The STE4 CCD was used with a Cousins R filter, 2 × 2 binning to decrease the readout time, and the telescope defocused. The resulting light curves have scatters of 1.5, 2.3, and 1.6 mmag. In the most recent run (2019 June) we cross-checked timings with another telescope at the observatory to confirm their reliability.

2.1 Data reduction

The raw data were reduced into light curves using the DEFOT pipeline (Southworth et al. 2009a, 2014) which implements aperture photometry, image motion tracking by cross-correlation with a reference image, and calculation of a differential-magnitude light curve. The light curve was obtained by simultaneously fitting the coefficients of a low-order polynomial versus time, and the weights of a set of comparison stars, to the data obtained outside transit. In all cases we used a linear or quadratic polynomial and the coefficients were included as fitted parameters in all subsequent analyses.

The best light curve was obtained by manually iterating the aperture sizes and which comparison stars were included – we found that the choices made here do affect the scatter of the light curve but have no significant effect on its shape. We did not perform bias or flat-field calibrations because they have a negligible effect on DFOSC data except for an increase in the noise level of the light curve (Southworth et al. 2014). All new data are shown in Fig. 1.

The timestamps were converted to the BJD(TDB) time-scale using routines from Eastman, Siverd & Gaudi (2010). Manual time checks were performed for images in most observing sequences, and no discrepancies were noticed.[1] We have previously found a good agreement between the timestamps on the Danish and MPG 2.2 m telescopes (Southworth et al. 2015), supporting the reliability of both.

Southworth et al. (2009b) used an early version of DEFOT so the 2008 data were re-reduced with the current version. This allowed the use of image motion tracking, additional comparison stars, and timestamps on the BJD(TDB) time-scale. The re-reduced data supersede those from Southworth et al. (2009b).

3 MEASUREMENTS OF THE TRANSIT TIMES

Each transit was fitted in isolation using the JKTEBOP[2] code (Southworth 2013, and references therein). The fitted parameters were the transit mid-point T_0, the fractional radii of the two components ($r_A = \frac{R_A}{a}$ and $r_b = \frac{R_b}{a}$ where R_A is the radius of the star, R_b is the radius of the planet, and a is the semimajor axis of the relative orbit) expressed as their sum and ratio, the orbital inclination, and the coefficients of the polynomial versus time. We modelled limb darkening using the quadratic law, fitted for the linear coefficient, and fixed the quadratic coefficient at an appropriate value.

Uncertainties on the transit times were obtained using Monte Carlo simulations and multiplied by $\sqrt{\chi_\nu^2}$ where χ_ν^2 is the reduced χ^2 of the fit. This final step is necessary because the aperture photometry routine used in our pipeline tends to underestimate the observational uncertainties. Table 1 gives the 22 transit times calculated in this work. To this data set we added all timings from table 2 of B19, which includes 41 measurements from the literature and 18 timings from the *TESS* light curve.

4 TRANSIT TIMING ANALYSIS

Our analysis was performed on the transit timings assembled above. We fitted a straight line to the times as a function of orbital cycle, using a zero-point for cycle number near to the mid-point of the available data to avoid correlations between the parameters of the ephemeris (Fig. 2). This yielded a poor fit so we tried a quadratic ephemeris instead, finding a significant improvement. The best-fitting linear ephemeris is

$$T_0 = \text{BJD(TDB)}\ 2\,456\,505.748953(20) + 1.338231429(20)E,$$

with $\chi_\nu^2 = 1.80$ and an rms scatter of 24.6 s. The bracketed quantities indicate the uncertainties in the preceding digits and have been increased by $\sqrt{\chi_\nu^2}$ to account for the imperfect fit. The best-fitting quadratic ephemeris is

$$T_0 = \text{BJD(TDB)}\ 2\,456\,505.749133(27) + 1.338231408(18)E - (1.95\pm0.23)\times 10^{-10}E^2,$$

with $\chi_\nu^2 = 1.41$ and an rms scatter of 19.9 s. As above, the uncertainties have been increased by $\sqrt{\chi_\nu^2}$ to account for the imperfect fit. We also fitted a cubic ephemeris but found it to be a negligible improvement on the quadratic ephemeris.

This quadratic coefficient corresponds to a period change of $\frac{dP}{dE} = (-3.91 \pm 0.46) \times 10^{-10}$ d per orbital cycle, and to a period derivative of

$$\frac{\mathrm{d}P}{\mathrm{d}t} = -9.2 \pm 1.1 \text{ ms yr}^{-1}.$$

This is roughly 3σ lower than the value of -12.6 ± 1.2 ms yr^{-1} found by B19. We investigated this by applying our analysis to only the transit times used by B19, which precisely reproduced their results. Therefore the difference in the period derivatives found by ourselves and by B19 is fully explained by the inclusion of additional transit times in this study.

The quadratic ephemeris has a much lower χ_ν^2 than the linear ephemeris. To explore this further we calculated the Bayesian Information Criterion (Schwarz 1978) to be 172.2 for the quadratic and 269.6 for the linear ephemeris, and the Akaike Information Criterion (Akaike 1974) to be 165.1 for the quadratic and 264.8 for the linear ephemeris. All three statistical quantities give a significant improvement for the quadratic versus the linear ephemeris, meaning that we have detected TTVs in the WASP-4 system. The quadratic term is negative and measured to 8.4σ significance.

The χ_ν^2 of our preferred quadratic ephemeris is significantly above unity. We have found this situation to occur for most transit timing studies both in our own experience (e.g. Southworth et al. 2016) and in published studies (e.g. Baluev et al. 2015; Maciejewski

[1]The 2009 season with the Danish Telescope suffered from a timing problem (Southworth et al. 2009c, 2010). We have investigated this further and found that it did not affect any observations of WASP-4 presented here.

[2]JKTEBOP is written in FORTRAN77 and the source code is available at http://www.astro.keele.ac.uk/jkt/codes/jktebop.html.

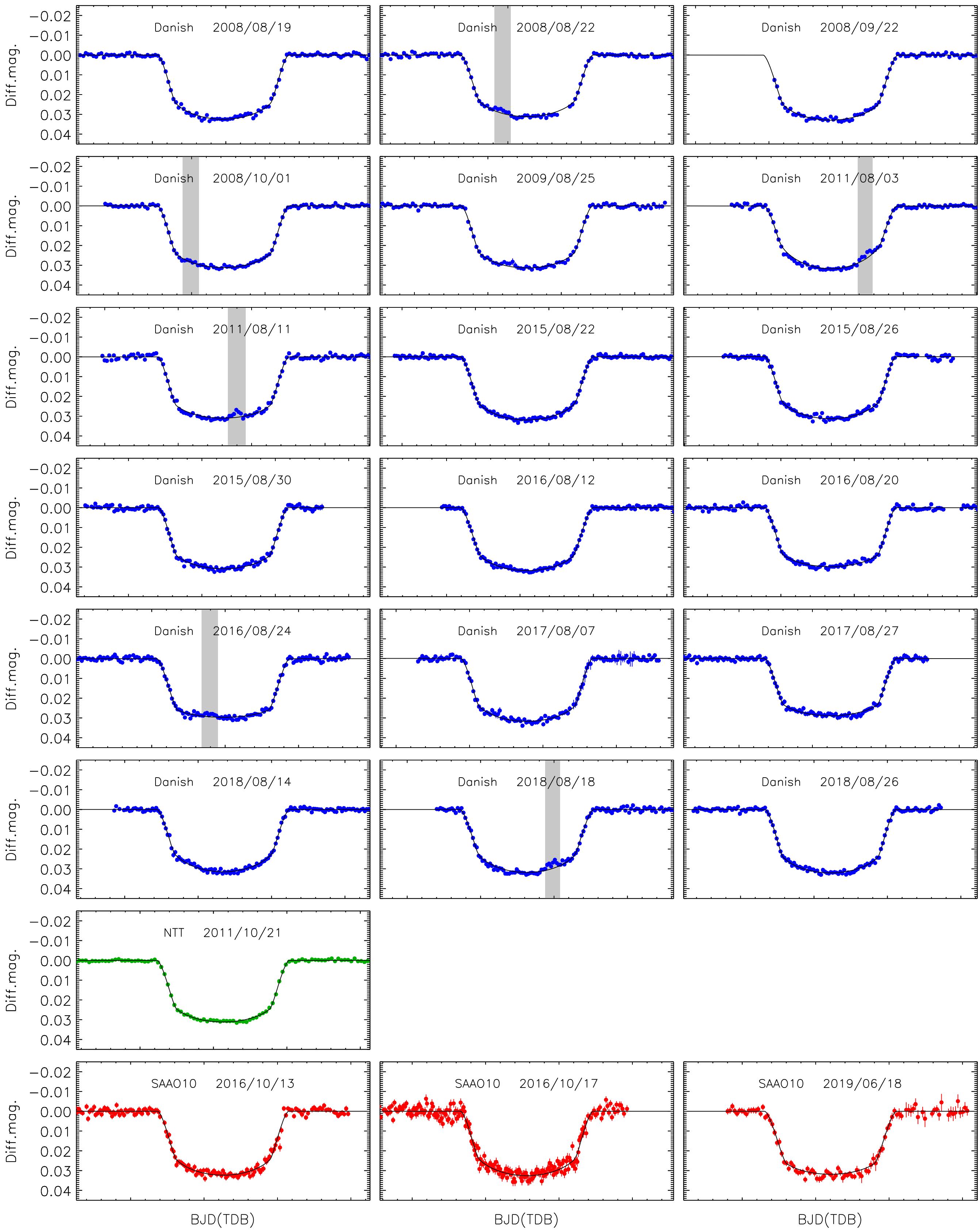

Figure 1. All new photometric data presented in this work. In each case the *x*-axis shows 0.2 d centred on the time of minimum measured for that transit. The telescope and date are labelled on each panel. Star-spot crossing events are visible during totality in six of the light curves, and are indicated by the grey boxes. The JKTEBOP best fits are shown using black lines.

Table 1. Times of mid-transit for WASP-4 determined in this work. The final column shows 'y' if spot crossings are clearly visible in the data.

Telescope	Date	Epoch	BJD(TDB)	Spot
Danish	2008-8-19	−1351	2454697.79821 ± 0.00010	
Danish	2008-8-22	−1348	2454701.81293 ± 0.00011	y
Danish	2008-9-22	−1325	2454732.59192 ± 0.00017	
Danish	2008-10-01	−1319	2454740.62150 ± 0.00007	y
Danish	2009-8-25	−1073	2455069.82652 ± 0.00009	
Danish	2011-8-03	−544	2455777.75045 ± 0.00014	y
Danish	2011-8-11	−538	2455785.78063 ± 0.00011	y
NTT	2011-10-21	−485	2455856.70662 ± 0.00007	
Danish	2015-8-22	562	2457257.83498 ± 0.00007	
Danish	2015-8-26	565	2457261.84940 ± 0.00010	
Danish	2015-8-30	568	2457265.86449 ± 0.00010	
Danish	2016-8-12	828	2457613.80465 ± 0.00010	
Danish	2016-8-20	834	2457621.83379 ± 0.00011	
Danish	2016-8-24	837	2457625.84865 ± 0.00010	y
SAAO 1.0 m	2016-10-13	874	2457675.36302 ± 0.00016	
SAAO 1.0 m	2016-10-17	877	2457679.37808 ± 0.00018	
Danish	2017-8-07	1097	2457973.78903 ± 0.00018	
Danish	2017-8-27	1112	2457993.86231 ± 0.00014	
Danish	2018-8-14	1375	2458345.81705 ± 0.00012	
Danish	2018-8-18	1378	2458349.83148 ± 0.00010	y
Danish	2018-8-26	1384	2458357.86123 ± 0.00008	
SAAO 1.0 m	2019-6-18	1605	2458653.61010 ± 0.00020	

et al. 2018a). The 8.4σ significance level of the quadratic term already includes an allowance for this large χ_ν^2. Fig. 2 shows that our new timings are consistent with published values in all cases where such a comparison can be drawn.

WASP-4 A shows star-spots and these are expected to add scatter to timing measurements both on theoretical (Ballerini et al. 2012; Oshagh et al. 2013) and empirical (Maciejewski et al. 2018b) grounds. The obvious outlier at cycle −544 and residual −64 s is affected by star-spots. To investigate this we rejected the six timings clearly affected by star-spot crossing events (Table 1) and recalculated the ephemerides. We find that the χ_ν^2 drops to 1.30 for the quadratic and 1.70 for the linear ephemeris, the quadratic term is not significantly changed, and its detection significance becomes 8.2σ. We conclude that spot activity increases the scatter of the transit timings but that TTVs are still detected to high confidence.

Visual inspection of Fig. 2 suggested the possibility of a sinusoidal variation superimposed on the quadratic term. We therefore calculated a periodogram of the residuals of the best fit to the quadratic ephemeris, using the PERIOD04 package (Lenz & Breger 2004). The periodogram contained no significant peaks, with the highest having a signal-to-noise ratio of 2.7. We find no significant peak near the period of 5.1 d tentatively identified by Baluev et al. (2015), so do not confirm this detection of sinusoidal variation. Further observations are needed to refine these conclusions.

5 POSSIBLE CAUSES OF THE TRANSIT TIMING VARIATION

In the previous section we have demonstrated that WASP-4 exhibits a quadratic variation in its transit times with a significance of 8.4σ. We now discuss possible causes of this effect.

5.1 Star-spots

Transit times measured from light curves exhibiting spot crossing events can be biased away from the true time of mid-point because the fitted model (transit of a planet across a limb darkened but otherwise uniform brightness star) is no longer adequate (Ballerini et al. 2012; Oshagh et al. 2013). The bias depends on where the spot crossing event is, with those near the start or end of a transit having the strongest effect (Oshagh et al. 2013). As activity levels on stars undergo cycles lasting years to decades (e.g. Baliunas et al. 1995), these effects could conceivably mimic a slow TTV. We have visually inspected all transits presented in this work in order to find those with clear spot crossing events. We have previously found visual methods to perform well in the identification of spot anomalies in transit light curves (Močnik, Southworth & Hellier 2017). We have indicated the transits with spot crossing events on Fig. 2, and find no clear correlation with the residuals versus the quadratic ephemeris fit. The quadratic term in the ephemeris is also detected to almost the same significance if these timings are rejected from the ephemeris fit.

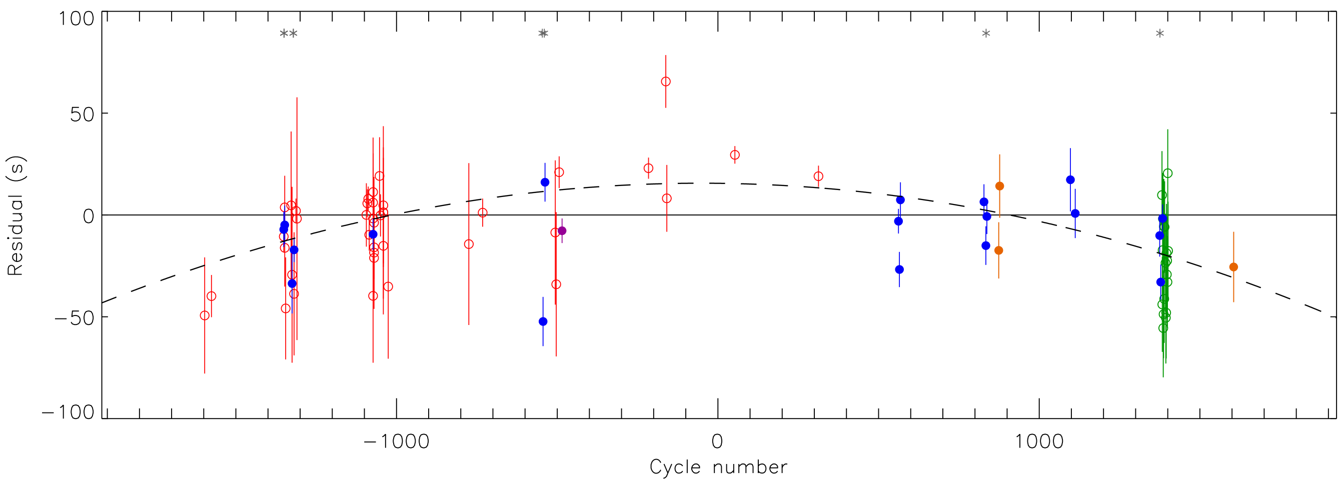

Figure 2. Plot of the residuals of the timings of mid-transit versus a linear ephemeris. The results from this work are shown with filled circles: blue for the Danish telescope, orange for the SAAO 1.0 m, and purple for the NTT. Published results are shown using open circles: red for the literature data collected by B19 and green for the *TESS* timings from B19. The dotted line shows the difference between the best-fitting linear and quadratic ephemerides. Grey asterisks have been placed near the top of the figure to indicate transit times measured from a light curve with a spot crossing event.

From Fig. 1 we see that star-spots are preferentially detected in WASP-4 towards the start or end of totality in the transit light curve. This is because the star-spots move with the stellar surface at an approximately constant angular speed, and thus at a variable linear speed when projected into the plane of the sky. The star-spots move faster when they are near the projected centre of the star, so are less likely to be found there. Conversely, smaller star-spots may be preferentially found away from the limb of the star because limb darkening will attenuate their photometric signal and make their detection less likely. Both effects should be accounted for in detailed statistical studies of these phenomena.

Watson & Dhillon (2004) investigated the effect of star-spots on timing measurements due to the Wilson depression: the phenomenon that star-spots are slightly depressed into the surface of the star. They found that this effect was sufficient to cause a change in the measured time of an eclipse at the level of a few seconds for a white dwarf plus M-dwarf binary. The effect will be less than a second for WASP-4 due to the larger radius ratio, so is not capable of causing the TTV we have found.

5.2 Applegate mechanism

Changes in the quadrupole moment of the star (Applegate 1992) have been proposed as a possible cause of TTVs in planetary systems. Watson & Marsh (2010) calculated the amplitude of the TTVs for WASP-4 for three scenarios concerning the length of the activity cycle in the host star. The largest TTV amplitude was found to be 15.3 s for a 50 yr activity cycle, so is a factor of six too small to explain the observed TTVs.

5.3 Orbital decay

Tidal effects will cause the majority of known hot Jupiters to merge with their host stars on a time-scale of several Gyr (Jackson, Barnes & Greenberg 2009; Levrard, Winisdoerffer & Chabrier 2009). This orbital decay will initially appear as a continuous decrease in their orbital period, causing a quadratic variation in the transit times. We followed the approach of Patra et al. (2017) to calculate the modified stellar tidal quality factor for the WASP-4 system, finding $Q'_\star = 10^{4.58\pm0.03}$.

A wide range of possible $Q'_\star$ values have been found in previous studies, both theoretical and observational. The canonical value of $Q'_\star$ is 10^6 (e.g. Ogilvie & Lin 2007), a value of $10^{5.5}$ was found to be a good match to a sample of extrasolar planets (Jackson, Greenberg & Barnes 2008), and a theoretical study by Essick & Weinberg (2016) yielded $Q'_\star \approx 10^5$ to 10^6 for short-period hot Jupiters. But other studies disagree: theoretical work by Penev & Sasselov (2011) constrained $Q'_\star$ to be 10^8–$10^{9.5}$, an observational study by Penev et al. (2012) found $Q'_\star > 10^7$, and Collier Cameron & Jardine (2018) used the distribution of orbital separations of the known population of transiting hot Jupiters to deduce $Q'_\star = 10^{8.26\pm0.14}$.

The value of $Q'_\star$ is also expected to depend on the nature of the tidal perturbation and the internal structure of the star (Ogilvie 2014; Penev et al. 2018), on orbital period (Barker 2011), and on planet mass (Barker & Ogilvie 2010). Barker (2011) found a dependence on orbital period of $Q'_\star \propto P^{14/5}$, giving a value of approximately $10^{5.3}$ for the WASP-4 system.

A tidal quality factor small enough to cause the TTV observed in WASP-4 is smaller than any determined in the observational and theoretical studies listed above. However, it is sufficiently close to the lower envelope of $Q'_\star$ values, and this envelope is sufficiently large, that it is not currently possible to rule out orbital decay as a cause of the TTV. Further work is needed to better understand the possible values of $Q'_\star$ and its dependence on system parameters such as planet mass and orbital period.

5.4 Light-time effect

The presence of a third component in the system on a wider orbit than WASP-4 b will cause a change in the measured transit timings due to the varying distance of the transiting system from the observer coupled with the finite speed of light.

As our data are adequately explained by a quadratic function, we can provide only speculative limits on the properties of a sinusoid that might also provide a good fit to the timings. To do so, we fit a linear ephemeris to all timings obtained before JD 2456600 and found that the most recent data arrived ∼100 s earlier than predicted by this ephemeris. As lower limits we adopted a period of triple the time interval covered by all of the timings, and an amplitude of 300 s. This yields a mass function of 2×10^{16} kg, giving a minimum mass of the putative third component of $\sim 2 \times 10^{-5}$ M$_\odot$ (0.02 M$_{\rm Jup}$). An object of this mass would have easily evaded spectroscopic detection, and at a minimum orbital separation of 0.6 au it would be much too close for detection via high-resolution imaging.

If present, this third object would imprint an orbital motion of amplitude ∼500 m s^{-1} on the radial velocity (RV) of the star. Knutson et al. (2014) searched for changes in the systemic velocity of WASP-4 A, finding an insignificant value of $\dot{\gamma} = -0.0099^{+0.0052}_{-0.0054}$ m s^{-1} d^{-1}. The 3σ upper limit on this is 5.9 m s^{-1} yr^{-1}, so would be 36 m s^{-1} over the 6-yr time interval covered by the RVs and 69 m s^{-1} over the 11.7-yr time interval covered by the transit timings. The lowest possible RV change over a 6-yr time interval is 67 m s^{-1}, 2 times larger than allowed by the 3σ upper limit on $\dot{\gamma}$, so the third-body interpretation is moderately inconsistent with the data.

Additional possibilities that could be invoked to bring the third-body hypothesis into better agreement with the data are orbital eccentricity (which must be sufficiently low to yield a roughly quadratic variation over the 11.7-yr interval covered by the available timings), an inclined orbit (which will not help much because it would require a larger third-body mass to obtain the same amplitude of the light-time effect), and a longer orbital period (which would also require a more massive third body). We conclude that the light-time effect is not a good explanation for the observed TTVs. Further analysis and RV measurements of the host star would help to strengthen this conclusion.

5.5 Apsidal motion

Patra et al. (2017) attempted to explain the quadratic orbital ephemeris of WASP-12 through apsidal precession, finding that it was consistent with the data but disfavoured relative to an orbital decay model. It is difficult to apply this model to WASP-4 because it requires measurements of the mid-point of occultations as well as transits over a significant time interval. Whilst some occultation timings are available (Beerer et al. 2011; Cáceres et al. 2011; Zhou et al. 2015) they lack the precision and time sampling necessary to provide useful constraints on apsidal motion in the system (see also B19). We recommend that new high-precision observations of occultations in the WASP-4 system are obtained.

Apsidal motion can only occur in eccentric systems. Triaud et al. (2010) found $e < 0.018$ for WASP-4 and Beerer et al. (2011) found $e\cos\omega = 0.00030 \pm 0.00086$: these do not constrain eccentricity sufficiently to rule out apsidal precession. One problem for this hypothesis, however, is the need for the system to have a non-zero eccentricity despite the presence of strong tidal effects in this short-period system containing a cool star with an extensive convective envelope.

6 SUMMARY

We have presented 22 times of mid-transit for the WASP-4 transiting planetary system that confirm the early arrival of transits noticed in *TESS* data (B19) and are consistent with a quadratic ephemeris. A constant orbital-period model is rejected at the 8.4σ significance level, making WASP-4 b only the third hot Jupiter with TTVs detected to high significance.

We have explored possible explanations for the observed TTVs. Instrumental timing effects cannot be blamed because there is good agreement between different telescopes in the same observing seasons, and they are also not apparent in any of the tests we have performed. Biases due to spot crossing events in the light curves have a negligible effect on our results so can be ruled out as the source of the TTVs. The Applegate mechanism gives TTVs a factor of six smaller than observed. The light-time effect due to a third body struggles to match our results. Apsidal precession is plausible and deserves further investigation, in particular the observation of secondary eclipses so the orbital period found from transits can be compared to that found from occultations.

Orbital decay is a plausible but not favourable option for causing the observed TTV. The tidal quality factor needed, $Q'_\star = 10^{4.58\pm0.03}$, is smaller than those predicted from theoretical arguments or measured from the population of known transiting planets. However, the envelope of possible values of $Q'_\star$ is broad and close to the value found for WASP-4, so it is not currently possible to discount this hypothesis.

A program of transiting timing measurements of a wide variety of planetary systems would help by providing observational constraints on orbital decay as a function of stellar type, planet mass, and orbital period. As $Q'_\star$ is expected to depend on the system parameters, it also would be interesting to perform TTV analyses on other systems similar to WASP-4. We used the TEPCat[3] catalogue (Southworth 2011) to identify HATS-2 and WASP-64 as the best candidates. These were found 5–6 yr later than WASP-4 so their transit timings cover a smaller time interval, but this could be compensated for by obtaining a larger number of high-quality transit observations in the near future.

We also advocate obtaining new observations of the WASP-4 system, and will be keeping it on the target list of the MiNDSTEp transit monitoring program. New transit times would refine and extend the baseline of the quadratic ephemeris. Further timings of secondary eclipses would allow the apsidal motion hypothesis to be ruled in or out. RV measurements of the planet host star would give stricter limits on the change in systemic velocity of the system. WASP-4 and WASP-12 stand out as the only hot Jupiters for which unexplained TTVs have been detected: as this phenomenon is uncommon it is reasonable to propose unusual or unlikely scenarios for such systems.

ACKNOWLEDGEMENTS

This paper uses data from the South African Astronomical Observatory (SAAO) under programmes Southworth-2016-05-1.0-m and Southworth-2019-01-40-inch-228, and from ESO under programme ID 088.C-0204 (P.I. Tregloan-Reed). The reduced light curves presented in this work will be made available at the CDS (http://cdsweb.u-strasbg.fr/) and at http://www.astro.keele.ac.uk/jkt/. We are grateful to Luke Bouma, Adrian Barker, and an anonymous referee for very useful comments that helped to significantly improve our paper. This project was partially funded by the MINEDUC-UA ESR project ANT 1795. The following internet-based resources were used in research for this paper: the ESO Digitized Sky Survey; the NASA Astrophysics Data System; the SIMBAD data base operated at CDS, Strasbourg, France; and the arχiv scientific paper preprint service operated by Cornell University.

Based on data collected by MiNDSTEp with the Danish 1.54 m telescope at the ESO La Silla Observatory.

[3]TEPCat (the Transiting Extrasolar Planet Catalogue) is available at http://www.astro.keele.ac.uk/jkt/tepcat/.

REFERENCES

Akaike H., 1974, IEEE Trans. Autom. Control, 19, 716
Applegate J. H., 1992, ApJ, 385, 621
Baliunas S. L. et al., 1995, ApJ, 438, 269
Ballerini P., Micela G., Lanza A. F., Pagano I., 2012, A&A, 539, A140
Baluev R. V. et al., 2015, MNRAS, 450, 3101
Barker A. J., 2011, MNRAS, 414, 1365
Barker A. J., Ogilvie G. I., 2010, MNRAS, 404, 1849
Becker J. C., Vanderburg A., Adams F. C., Rappaport S. A., Schwengeler H. M., 2015, ApJ, 812, L18
Beerer I. M. et al., 2011, ApJ, 727, 23
Birkby J. L. et al., 2014, MNRAS, 440, 1470
Bouma L. G. et al., 2019, AJ, 157, 217 (B19)
Buzzoni B. et al., 1984, Messenger, 38, 9
Cáceres C. et al., 2011, A&A, 530, A5
Collier Cameron A., Jardine M., 2018, MNRAS, 476, 2542
Dominik M. et al., 2010, Astron. Nachr., 331, 671
Eastman J., Siverd R., Gaudi B. S., 2010, PASP, 122, 935
Essick R., Weinberg N. N., 2016, ApJ, 816, 18
Evans D. F. et al., 2016, A&A, 589, A58
Gibson N. P. et al., 2010, MNRAS, 401, 1917
Harpsøe K. B. W. et al., 2013, A&A, 549, A10
Holman M. J., Murray N. W., 2005, Science, 307, 1288
Jackson B., Greenberg R., Barnes R., 2008, ApJ, 678, 1396
Jackson B., Barnes R., Greenberg R., 2009, ApJ, 698, 1357
Knutson H. A. et al., 2014, ApJ, 785, 126
Lenz P., Breger M., 2004, in Zverko J., Žižnovsky J., Adelman S. J., Weiss W. W., eds, Proc. IAU Symp. 224, The A-Star Puzzle. Cambridge Univ. Press, Cambridge, UK, p. 786
Levrard B., Winisdoerffer C., Chabrier G., 2009, ApJ, 692, L9
Maciejewski G. et al., 2016, A&A, 588, L6
Maciejewski G., Stangret M., Ohlert J., Basaran C. S., Maciejczak J., Puciata-Mroczynska M., Boulanger E., 2018a, Inf. Bull. Var. Stars, 6243
Maciejewski G. et al., 2018b, Acta Astron., 68, 371
Mazeh T. et al., 2013, ApJS, 208, 16
Mortier A., Santos N. C., Sousa S. G., Fernandes J. M., Adibekyan V. Z., Delgado Mena E., Montalto M., Israelian G., 2013, A&A, 558, A106
Močnik T., Southworth J., Hellier C., 2017, MNRAS, 471, 394
Ngo H. et al., 2015, ApJ, 800, 138
Ogilvie G. I., 2014, ARA&A, 52, 171
Ogilvie G. I., Lin D. N. C., 2007, ApJ, 661, 1180
Oshagh M., Santos N. C., Boisse I., Boué G., Montalto M., Dumusque X., Haghighipour N., 2013, A&A, 556, A19
Patra K. C., Winn J. N., Holman M. J., Yu L., Deming D., Dai F., 2017, AJ, 154, 4
Penev K., Sasselov D., 2011, ApJ, 731, 67
Penev K., Jackson B., Spada F., Thom N., 2012, ApJ, 751, 96
Penev K., Bouma L. G., Winn J. N., Hartman J. D., 2018, AJ, 155, 165
Ricker G. R. et al., 2015, J. Astron. Telesc. Instrum. Syst., 1, 014003

Sanchis-Ojeda R., Winn J. N., Holman M. J., Carter J. A., Osip D. J., Fuentes C. I., 2011, ApJ, 733, 127
Schwarz G., 1978, Ann. Stat., 5, 461
Southworth J., 2011, MNRAS, 417, 2166
Southworth J., 2012, MNRAS, 426, 1291
Southworth J., 2013, A&A, 557, A119
Southworth J. et al., 2009a, MNRAS, 396, 1023
Southworth J. et al., 2009b, MNRAS, 399, 287
Southworth J. et al., 2009c, ApJ, 707, 167
Southworth J. et al., 2010, ApJ, 723, 1829
Southworth J. et al., 2014, MNRAS, 444, 776
Southworth J. et al., 2015, MNRAS, 447, 711
Southworth J. et al., 2016, MNRAS, 457, 4205
Tregloan-Reed J., Southworth J., 2013, MNRAS, 431, 966
Triaud A. H. M. J. et al., 2010, A&A, 524, A25
Watson C. A., Dhillon V. S., 2004, MNRAS, 351, 110
Watson C. A., Marsh T. R., 2010, MNRAS, 405, 2037
Wilson D. M. et al., 2008, ApJ, 675, L113
Woltjer J. J., 1922, Bull. Astron. Inst. Neth., 1, 93
Zhou G., Bayliss D. D. R., Kedziora-Chudczer L., Tinney C. G., Bailey J., Salter G., Rodriguez J., 2015, MNRAS, 454, 3002

[1]*Astrophysics Group, Keele University, Staffordshire ST5 5BG, UK*
[2]*Centre for Exoplanet Science, SUPA, School of Physics & Astronomy, University of St Andrews, North Haugh, St Andrews KY16 9SS, UK*
[3]*Niels Bohr Institute & Centre for Star and Planet Formation, University of Copenhagen, Øster Voldgade 5, DK-1350 Copenhagen, Denmark*
[4]*Niels Bohr Institute, Blegdamsvej 17, DK-2100 Copenhagen, Denmark*
[5]*Dipartimento di Fisica 'E.R. Caianiello', Università di Salerno, Via Giovanni Paolo II 132, I-84084 Fisciano, Italy*
[6]*Istituto Nazionale di Fisica Nucleare, Sezione di Napoli, Napoli, Italy*
[7]*Department of Earth Sciences, Meteorological Institute, Universität Hamburg, Bundesstraße 55, D-20146 Hamburg, Germany*
[8]*Instituto de Astrofísica, Facultad de Física, Pontificia Universidad Católica de Chile, Av. Vicuña Mackenna 4860, 7820436 Macul, Santiago, Chile*
[9]*Laboratoire d'Astrophysique de Bordeaux, Université de Bordeaux, CNRS, B18N, allée Geoffroy Saint-Hilaire, F-33615 Pessac, France*
[10]*Max Planck Institute for Astronomy, Königstuhl 17, D-69117 Heidelberg, Germany*
[11]*Facultad de Ingeniería y Tecnología Universidad San Sebastían, General Lagos 1163, 5110693 Valdivia, Chile*
[12]*Institute for Advanced Research and Department of Physics, Nagoya University, Furo-cho, Chikusa-ku, 464-8601 Nagoya, Japan*
[13]*Department of Physics, University of Warwick, Gibbet Hill Road, Coventry CV4 7AL, UK*
[14]*Instituto de Astronomía y Ciencias Planetarias de Atacama, Universidad de Atacama, Copayapu 485, Copiapo, Chile*
[15]*Department of Astronomy and Space Science, Chungnam National University, 34134 Daejeon, Republic of Korea*
[16]*Department of Physics, Sharif University of Technology, PO Box 11155-9161 Tehran, Iran*
[17]*DARK, Niels Bohr Institute, University of Copenhagen, Lyngbyvej 2, DK-2100 Copenhagen, Denmark*
[18]*Centro de Astronomía (CITEVA), Universidad de Antofagasta, Avda. U. de Antofagasta 02800, Antofagasta, Chile*
[19]*Department of Physics, University of Rome Tor Vergata, Via della Ricerca Scientifica 1, I-00133 Rome, Italy*
[20]*INAF – Osservatorio Astrofisico di Torino, via Osservatorio 20, I-10025 Pino Torinese, Italy*
[21]*International Institute for Advanced Scientific Studies (IIASS), Via G. Pellegrino 19, I-84019 Vietri sul Mare (SA), Italy*
[22]*CITEUC – Center for Earth and Space Science Research of the University of Coimbra, 3040-004 Coimbra, Portugal*
[23]*Las Cumbres Observatory Global Telescope, 6740 Cortona Dr., Suite 102, Goleta, CA 93111, USA*
[24]*Department of Physics, University of California, Santa Barbara, CA 93106-9530, USA*
[25]*Department of Physics, Isfahan University of Technology, Isfahan 84156-83111, Iran*
[26]*Centre for Electronic Imaging, Department of Physical Sciences, The Open University, Milton Keynes MK7 6AA, UK*
[27]*Institute for Astronomy, University of Edinburgh, Royal Observatory, Edinburgh EH9 3HJ, UK*
[28]*Stellar Astrophysics Centre, Department of Physics and Astronomy, Aarhus University, Ny Munkegade 120, DK-8000 Aarhus C, Denmark*

This paper has been typeset from a TEX/LATEX file prepared by the author.